AIAA JOURNAL
Vol. 48, No. 1, January 2010

Subatmospheric Extinction of Opposed-Jet Diffusion Flames of Jet Fuel and Its Surrogates

Srinivasan Dattarajan,* Okjoo Park,† Elizabeth M. Fisher,‡ and Frederick C. Gouldin§
Cornell University, Ithaca New York 14853
and
Joseph W. Bozzelli¶
New Jersey Institute of Technology, Newark, New Jersey 07102

DOI: 10.2514/1.42742

In this experimental study, the pressure dependence of the extinction strain rate of flames of jet fuel and other hydrocarbons was measured and quantified. Laminar nonpremixed opposed-jet flames of fuel/nitrogen mixtures versus oxygen-enriched air were progressively strained to extinction by lowering pressure over the pressure range 0.1 to 0.68 atm. The fuels investigated were methane; ethylene; Jet-A; *n*-decane; 1, 2, 4-trimethyl benzene; and blends of *n*-decane and 1, 2, 4-trimethyl benzene. All liquid fuels were vaporized and diluted to a mass fraction of 21.5% in nitrogen gas; the gaseous fuels were not diluted. The oxidizer was a 50/50% molar mixture of oxygen and nitrogen. The global strain rate at extinction was seen to monotonically increase with pressure in the subatmospheric pressure range explored. Overall reaction orders calculated from density-weighted extinction strain rates were between 1.3 and 2.0. Jet-A flames were extinguished at conditions similar to those for the decane/trimethyl benzene blends, indicating that these blends can serve as a surrogate for Jet-A.

I. Introduction

COMPLEX liquid fuels, consisting of myriad components belonging to multiple classes of hydrocarbons, are the norm in practical combustion devices and have recently received heightened attention in the combustion community. Several recent studies [1–4] have focused on the development of surrogate mixtures with a limited number of components that can be used to simulate the behavior of practical fuels such as jet fuel, diesel, and gasoline. Surrogate development becomes challenging when both physical properties (such as volatility and viscosity) and chemical characteristics (such as kinetics in various regimes and thermochemistry) must be matched. It is a common practice to select one or more reference fuels from each major class of hydrocarbons present (e.g., normal alkanes, aromatics, branched alkanes, etc.) and adjust proportions of these reference fuels to match desired properties.

In the current study, we investigate the flame extinction behavior of two reference fuels and compare the behavior of the reference fuels and their blends with that of jet fuel. This approach is similar to the use of binary blends of reference fuels to match a single combustion characteristic (knock) for automotive fuels. The two reference fuels of the current study are the low-octane, reactive, and relatively hard to extinguish *n*-decane and the relatively nonreactive, high-octane, and easy to extinguish 1, 2, 4-trimethyl benzene (TMB). Specifically, we determine extinction strain rate as a function of pressure for nonpremixed flames of Jet-A, the two reference fuels, and two blends of the reference fuels in an opposed-jet burner over the pressure range 0.29 to 0.68 atm. We also include measurements with pure methane and ethylene for comparison, over a different pressure range. Liquid phase and vaporization properties of the fuels are not investigated, as the liquid fuels are vaporized and mixed with nitrogen before delivery to the burner in our experiments. The strain rate at extinction in an opposed-jet diffusion flame is a fundamental kinetic property against which chemical kinetic mechanisms can be tested using a simple one-dimensional flame model; furthermore, the behavior of strained laminar flames is relevant to local extinction of flamelets in practical turbulent combustion devices [5,6].

One developing application of lower-pressure combustion is in scramjets. Although hydrogen has fueled initial scramjet demonstrations, hydrocarbon combustion in scramjets holds significant advantages in terms of ease and safety of operational handling [7,8], cooling [9], etc. Because of their high flight altitudes, the combustor inlet static pressures of scramjet engines can be as low as 0.1 atm [10,11]. These low pressures put some combustion reactions in the fall-off regime, necessitating the use of pressure-dependent kinetic parameters [12].

The pressure dependence of extinction strain rates has previously been studied for nonpremixed flames with gaseous fuels. Law [13] discusses the influence of elevated pressure on various combustion phenomena including extinction and argues that for diffusion flames, density-weighted strain rates more accurately characterize extinction behavior, owing to the relative independence of density-weighted diffusivities with pressure. Numerical studies of diluted hydrogen flames [14,15] predict a complex pressure dependence of extinction strain rate, with strain rates increasing with pressure at low pressures, then decreasing, and finally increasing again at high pressures. This behavior reflects the well-known pressure dependence of the competition between chain branching and chain termination reactions involving HO_2 [16]. Methane extinction has been studied as a function of pressure both numerically [17,18] and experimentally [18,19]. For pure CH_4 vs pure O_2, Pons et al. [17] predict a monotonic increase in extinction strain rate with pressure, up to a pressure of 150 atm. Qualitatively similar observations and predictions are made by Chelliah et al. [18] for methane/air flames at pressures between 0.25 and 2.5 atm. In both cases, the rate of increase of extinction strain rate with pressure decreases as pressure increases. Experiments with two different highly diluted methane vs air flames over the range

Presented at the 47th AIAA Aerospace Sciences Meeting, Orlando, FL, 5–8 January 2009; received 15 December 2008; revision received 20 September 2009; accepted for publication 21 September 2009.

*Postdoctoral Associate, Sibley School of Mechanical and Aerospace Engineering; currently Lead Engineer, GE Aviation, Bangalore, India.
†Visiting Scientist, Sibley School of Mechanical and Aerospace Engineering; currently Graduate Student Researcher, University of Southern California.
‡Associate Professor, Sibley School of Mechanical and Aerospace Engineering; emf4@cornell.edu.
§Professor, Sibley School of Mechanical and Aerospace Engineering; Associate Fellow AIAA.
¶Professor, Department of Chemistry and Environmental Science.

1–4 atm show different behavior: extinction strain rates are observed to be virtually independent of pressure in one case and have a maximum near a pressure of 2 atm in the other.

Law [19] examines pressure dependence of extinction strain rates through an asymptotic analysis of nonpremixed counterflow flames involving generic chain branching and chain termination reactions. He concludes that the density-weighted extinction strain rate should be approximately proportional to pressure to the overall reaction order. If reactions are modeled through a one-step overall reaction, the pressure dependence should be approximately quadratic. Law [19] observes lower overall reaction orders experimentally and interprets them as indicating the increasing importance of three-body termination reactions as pressure increases, an effect that tends to occur more readily at lower temperatures. Chelliah et al. [18] estimate global reaction order for methane/air flames from the density-scaled extinction strain rates. The reaction order is found to decrease gradually from 1.96 at low pressures to 1.45 at high pressures. In agreement with the discussion of hydrogen flames described above, Chelliah et al. [18] attribute the decrease in reaction order with pressure to the increasing importance of chain termination reactions, especially the one forming HO_2.

Our study investigated the pressure dependence of extinction strain rates of vaporized Jet-A and its surrogates in the subatmospheric pressure regime because of the applicability of this regime to scramjet combustors. To our knowledge, the effect of pressure on the extinction strain rate of vaporized liquid fuels has not been studied.

II. Apparatus and Method

Figure 1 shows a schematic diagram of the opposed-jet burner used for the current experiments, which consisted of two coaxial open stainless steel tubes, one carrying fuel and the other carrying oxidizer, housed in a vacuum chamber. The i.d. of the tubes and axial distance between their exits (i.e., the tube gap size) were both 1 cm. Fuel was delivered through the upper burner tube, and oxidizer was delivered from below. The opposing fuel and oxidizer jets, of nearly equal momentum flux, collided in the gap between the burner tubes, resulting in the formation of a stagnation plane, near which a diffusion flame could be sustained. In order to prevent the formation of secondary flames, nitrogen gas was passed through the annuli between the burner tubes and outer sheath tubes on the fuel and oxidizer sides. The products of combustion were drawn out of the vacuum chamber by a Stokes rotary piston pump. For a given set of reactant and sheath nitrogen flow rates, the pressure in the chamber could be modulated by a flow metering valve on the vacuum chamber's exhaust line. The pressure in the chamber was measured with a capacitance manometer.

The liquid fuels were vaporized into a heated stream of nitrogen carrier gas. They were metered by a syringe pump and delivered to a concentric glass nebulizer manufactured by Meinhard, Inc. (Golden, Colorado). Test data for droplet size variation with flow rate provided by the manufacturer and suitably corrected for the physical properties of the fuels indicate that a fine mist of droplets of nominal diameter between 3.5 and 25 μm was produced, depending on the fuel flow rate. These droplets were injected into a vaporization chamber and allowed to vaporize into a stream of coflowing preheated nitrogen. This mixture of fuel vapor and nitrogen carrier gas constituted the fuel mixture. The pressure in the vaporization chamber was controlled to approximately 1 atm via a metering valve installed between the vaporization chamber and the main vacuum chamber. Previous low-pressure experiments, conducted before this pressure control was installed, had shown evidence of air leakage into the syringe and corresponding inaccuracies in measured liquid fuel flow rate.

The oxidizer stream comprised an equimolar mixture of oxygen and nitrogen. The gases in both fuel and oxidizer streams were metered using mass flow controllers. The fuel and air delivery lines and the vaporization chamber were heated with electrical heating tapes. Heating was done to maintain the fuel and oxidizer jet exits at fixed temperatures, as described below, and to prevent recondensation of fuel vapors in the case of liquid fuels. The calculated residence time of the fuel droplets in the heated vaporization chamber and delivery lines was much higher than the estimated time needed for the droplets to fully vaporize. For a given flow rate of liquid at the syringe pump, the flow rate of the nitrogen carrier gas was adjusted to

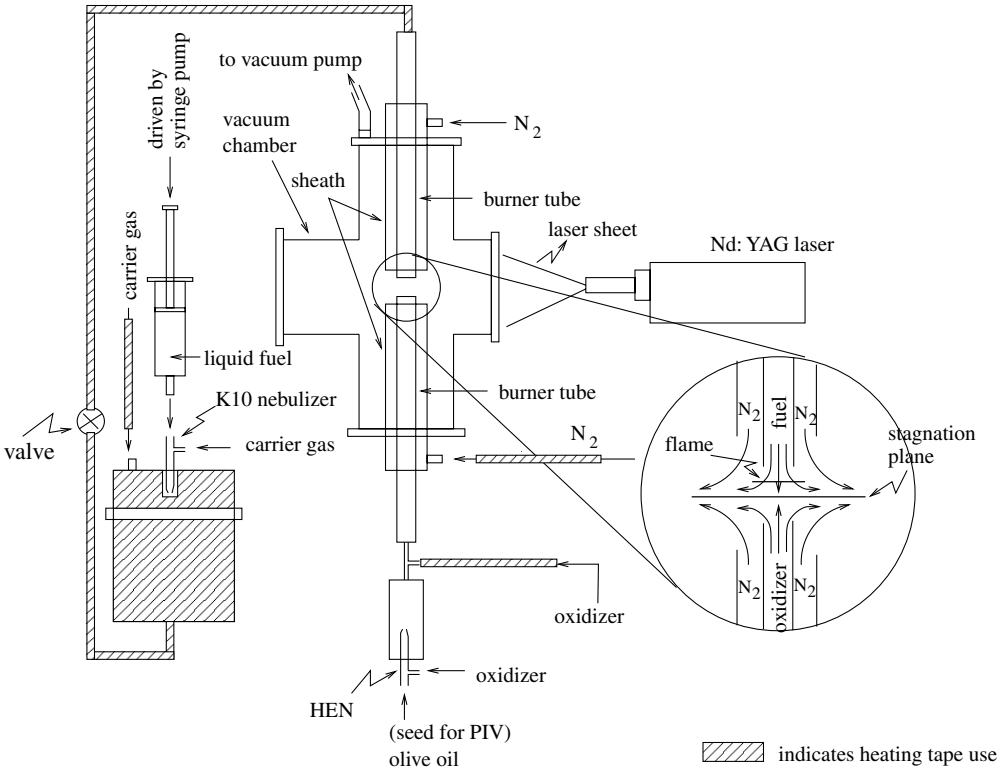

Fig. 1 Schematic of the opposed-jet diffusion flame apparatus.

give the desired fuel-side composition, and the flow rate of oxidizer was then adjusted to produce a jet of the same momentum flux as that of the fuel jet.

The temperatures of the fuel and oxidizer jets were measured using K-type unsheathed thermocouple wires 0.0762 mm in diameter and mounted along chords of the respective tubes, 2.54 cm upstream of the respective tube exits. Velocity field measurements, to be discussed below, indicated minimal disturbance to the flow owing to the presence of the thermocouple wires. These measured temperatures were fed back to temperature controllers, which maintained the fuel- and oxidizer-side exit temperatures at 150 and 100°C, respectively, with the aid of heating tapes wrapped around the fuel and air delivery lines. The entire fuel line was maintained hot in order to prevent recondensation of the fuel vapors. Jet fuels have been observed [20] to decompose on heated surfaces; however, we found no evidence of such decomposition in our system. In order to investigate this possibility, we used a Thermo Fisher gas chromatograph/mass spectrometer (GC/MS) to analyze the composition of a liquid jet fuel sample and compared it to that of a vaporized jet fuel sample obtained at the burner-tube exit. This test was done on one occasion to check whether the jet fuel's composition changed by the time it reached the burner exit. Because the different physical form of the sample necessitated different GC/MS methods, a quantitative comparison of species mole fractions was not meaningful. The chromatograms from the two samples, as seen in Fig. 2, show that the same pattern of elution times is obtained from the two samples. Note that in Fig. 2 each chromatogram is normalized by the magnitude of the largest peak in the time range shown. Mass spectra were used to identify the species responsible for the major peaks, which were the same for the two samples. Thus, there was no evidence of jet fuel decomposition to form new compounds not present in the original fuel.

In some of the experiments, the oxidizer-side velocity field was measured using particle image velocimetry (PIV). Olive oil droplets of nominal diameter 3.5 μm, generated in a high-efficiency nebulizer (Meinhard), were used as seeding particles; the heating value of the seed particles in the oxidizer stream was negligible compared to that of the fuel in the fuel stream. The droplet diameter that resulted from the natural aspiration of water by the nebulizer, when the latter was operated at its design gas-phase pressure, was provided by the manufacturer and is reported here as nominal diameter. A pair of Nd:YAG lasers with maximum pulse energies of 120 mJ/pulse, operating at 5 Hz, were used to illuminate the PIV particles. A charge-coupled device camera with 1360×1036 pixel resolution acquired image pairs, which were then processed with a cross-correlation scheme to obtain velocity vectors using the freely available MatPIV [21] software.

Representative velocity profiles measured using PIV are shown in Fig. 3. Figure 3a shows the measured velocity profile at the oxidizer jet exit, with the fuel jet turned off. The chamber was at atmospheric pressure. The volume flow rate calculated by integrating a parabolic fit to the exit velocity profile over the burner-tube cross-sectional area agreed with the flowmeter reading within measurement accuracy.

Figure 3b shows radial profiles of axial velocity 0.2 mm downstream of the burner exit, compared to parabolic profile giving the same flow rate. These profiles were obtained during burner operation with a flame, near extinction. The fuel was an 80/20 blend of *n*-decane and TMB heated to 150°C, and the oxidizer was a 50/50 blend of oxygen and nitrogen, heated to 100°C. The strain rate and pressure were 691 s^{-1} and 334 torr, respectively; extinction was subsequently

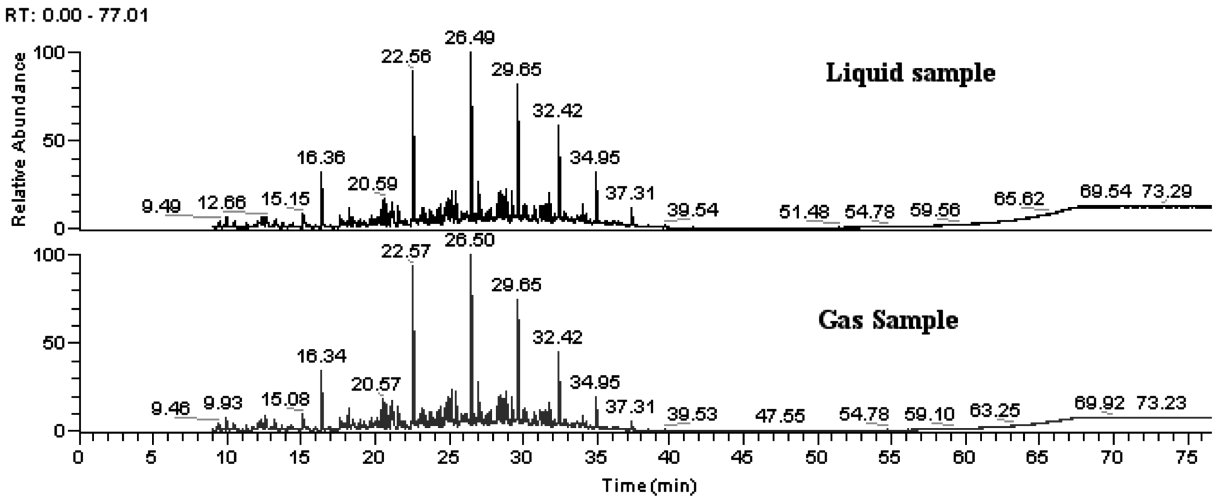

Fig. 2 Chromatograms (total ion count) for liquid and vaporized jet fuel samples. Numbers indicate peak elution times, as determined by GC/MS software.

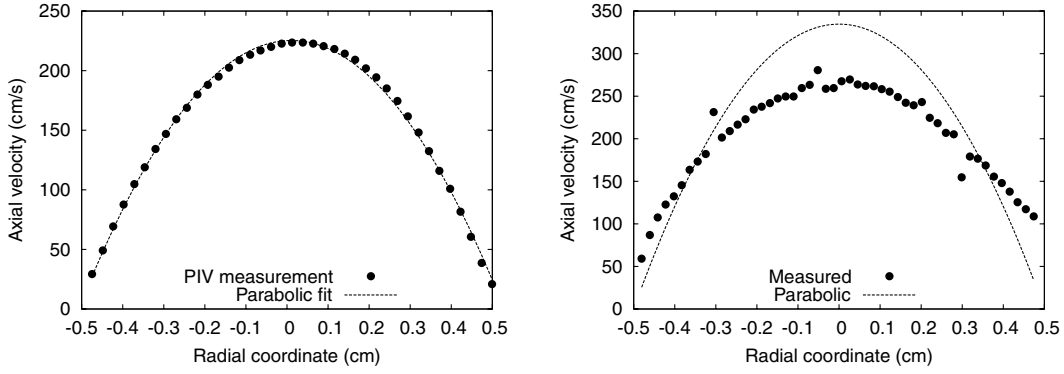

a) **b)**

Fig. 3 Radial profile of the jet axial velocity 0.2 mm downstream of the oxidizer tube exit a) in the absence of combustion and b) during combustion.

reached at 709 s^{-1} and 324 torr. As expected, the profiles are somewhat flattened from the parabolic profile that one would obtain in the absence of the other jet and the flame, consistent with the observation of Chelliah et al. [18] that flow profiles at the jet exit in many opposed-jet experimental studies more closely resemble plug flow than a parabolic velocity profile. The Reynolds numbers based on the oxidizer jet bulk speed and the burner-tube i.d. were in the range of 400–1800 for the experiments conducted in this study.

For a given set of reactant flow rates, the global strain rate is given by [22]

$$a_q = \frac{2V_O}{L}\left(1 + \frac{V_F}{V_O}\sqrt{\frac{\rho_F}{\rho_O}}\right) \quad (1)$$

where V_F and V_O are the volume average fuel and oxidizer jet exit velocities, L is the gap size, and ρ_F and ρ_O are the jet exit densities of the fuel and oxidizer, respectively. The global strain rate is quantified using globally measured quantities such as reactant flow rates and burner geometry. The strain rates reported in Sec. V are all global strain rates and were determined using Eq. (1). A local strain rate can be defined as the maximum absolute value of the axial gradient of axial velocity on the oxidizer side of the flame. Though local strain rates are not reported in this study, a linear correlation between global and local strain rates can be found in Zegers et al. [23], wherein the burner used is almost identical to that of the current study.

For a given set of fuel and oxidizer flow rates, the jets were heated to the desired exit temperatures. Once a diffusion flame was established in the gap between the burner tubes, it was progressively strained by manually reducing the chamber pressure. This was achieved by gradually opening the flow metering valve between the vacuum chamber and the vacuum pump while maintaining the reactant mass flow rates constant. Because extinction needed to be approached quasi-steadily, the decrease in pressure was brought about very gradually at chamber pressures within 20 torr of the anticipated extinction pressure. The entire process typically took approximately 30 min for each data point. The pressure in the chamber just before extinction is reported here as extinction pressure.

III. Materials and Operating Conditions

Though the focus of our study is on Jet-A and surrogates composed of decane and TMB, extinction measurements were also performed on methane and ethylene flames. Table 1 lists the chemicals used in the current experiments, along with their sources and purities.

Table 2 lists the operating conditions of the experiments. The oxidizer stream was a 50/50% molar mixture of N_2 and O_2, at 100°C. The fuel stream was at 150°C. Fuel and oxidizer flow rates were chosen to provide equal momentum fluxes. The liquid fuels were vaporized into nitrogen gas such that the fuel mass fraction in the fuel stream was 0.215. For the liquid fuel experiments, we chose to match the mass fraction of the fuel in the fuel stream among the different tests done. Also shown in Table 2 are two indicators of flame temperature and position: the adiabatic flame temperature for a stoichiometric mixture of the fuel stream and oxidant stream, at 1 atm, and the stoichiometric mixture fraction, or mass fraction of material from the fuel stream that is found at the stoichiometric contour. The similar values among the liquid fuels tested here indicate that the fuels were being tested under comparable conditions.

IV. Error Estimation

The quantities measured directly to evaluate the expression for global extinction strain rate in Eq. (1) were the fuel, carrier nitrogen, and oxidizer flow rates; the fuel- and air-side temperatures; burner geometric parameters; and the pressure in the vacuum chamber at extinction. The precision uncertainty (i.e., random error) associated with each type of measurement is listed in Table 3. The uncertainty estimate is based on manufacturers specifications for measurements of temperature, flow rates, and pressure. It is based on the standard deviation of repeated measurements in the case of burner geometry measurements. These errors combine to produce uncertainties in the strain rates obtained from the raw measurements. In this section, we describe the process for calculating the impact of the uncertainties in the raw measurements on the uncertainty in the calculated strain rate and indicate the magnitude of the resulting uncertainty.

Table 1 Chemicals used

Reactant	Use	Source	Purity and/or Composition
Methane	Fuel	Air gas	Chemically pure, 99.9% minimum purity
Ethylene	Fuel	Air gas	Grade 2.5, 99.5% purity
n-decane used in pure *n*-decane experiments	Fuel	EMD chemicals (Merck)	98% minimum purity
n-decane used in blends	Fuel	Fisher Scientific	99.9% purity
Trimethyl benzene	Fuel	Tokyo Kasei Kogyo Co., Ltd.	98% purity
Jet-A	Fuel	AFRL (batch #Posf 4658)	As described in Holley et. al. [4]: 4658 Jet-A blend
O_2/N_2 mixture	Oxidizer	Air gas	Primary Standard: 50% O_2; balance N_2. Analytical uncertainty: ±0.01
Nitrogen	Fuel stream component; annular sheath gas	Air gas	Industrial grade; >99.998% typical purity

Table 2 Test conditions for opposed-jet diffusion flame experiments

Fuel stream	Adiabatic flame temperature, K	Stoichiometric mixture fraction	Pressure range of extinction experiments, atm
Gaseous fuels			
Pure methane	2828	0.12	0.10–0.28
Pure ethylene	2941	0.13	0.12–0.21
Liquid fuels			
Decane	2627	0.42	0.33–0.68
Decane/TMB blend in the proportion 80/20 by liquid volume	2629	0.42	0.30—0.55
Decane/TMB blend in the proportion 60/40 by liquid volume	2631	0.42	0.46–0.59
Jet-A	2609	0.45	0.29–0.59
Trimethylbenzene	2636	0.44	0.59–0.86

Table 3 Precision uncertainty estimates for instruments used in the experiments

Quantity being measured	Instrument	Typical precision uncertainty
Temperature	Thermocouple	2°C
Liquid fuel flow rate	Syringe pump	1%
Gaseous reactant flow rate	Mass flow controller	1% of full scale
Pressure	Capacitance manometer	1 torr
Burner-tube diameter	Calipers	0.06 mm
Burner-tube gap size	Calipers	0.25 mm

Denoting the raw measurements as X_1, X_2, etc., and the precision uncertainties associated with them as ΔX_1, ΔX_2, etc., we propagate errors to obtain Δa_q, the precision uncertainty in extinction strain rate a_q as follows:

$$\Delta a_q = \left[\sum_i \left(\frac{\partial a_q}{\partial X_i}\Delta X_i\right)^2\right]^{1/2} \tag{2}$$

In order to obtain an error representing the point-to-point scatter in the data points, we omitted the burner geometry precision error from the calculation. Geometric parameters were not measured independently for each data point; rather, they were measured several times, values were averaged, and then the resulting numbers were used for processing all data points. Thus, any error in measurements of gap size and burner diameter would result in a shift of all data points in the same direction, not a point-to-point scatter.

This estimate of precision error in extinction strain rate depended on the fuel being used and the exact operating conditions. For the liquid fuel experiments reported here, it ranged from 1–3%, with the highest fractional uncertainties occurring at the lower end of the pressure range explored for a given fuel. In absolute terms, this corresponds to an error in the extinction strain rate of ± 8 to ± 16 s^{-1}, or roughly the size of the symbols used in the figures of the following section. If burner geometry contributions to uncertainty are included, the uncertainty in extinction strain rate ranges from ± 18 to ± 32 s^{-1}. Absolute uncertainties (i.e., uncertainties expressed as strain rates rather than percentages) are larger for methane and ethylene measurements, but again roughly comparable to the size of the symbols used to represent data points.

The same error propagation analysis can be performed to estimate precision errors associated with the mass fraction values of liquid fuels in the fuel stream. In this case the precision error ranges from 1 to 3.5% of the fuel mass fraction. Note that the impact of the uncertainty in fuel stream composition on the scatter in extinction strain rate has not been evaluated.

V. Results and Discussion

As noted in Sec. II, after establishing a flame between the burner tubes, the pressure in the vacuum chamber was reduced quasi-steadily until extinction, and the pressure just before extinction was recorded as the extinction pressure. In this section, quantitative data on the dependence of the global extinction strain rate a_q on pressure are presented.

A. Extinction Strain Rates

Undiluted methane and ethylene were the gaseous fuels tested in this study, as shown in Table 2. The dependence of the extinction strain rate for these fuels on pressure is shown in Fig. 4. In both cases, extinction strain rate increases approximately linearly with pressure. Ethylene exhibits a substantially higher extinction strain rate than methane does at a given pressure, in agreement with observations at atmospheric pressure of previous investigators [24].

Similar measurements were carried out previously for methane and ethylene, but with air as the oxidizer and neither fuel nor air streams being heated. The results are reported elsewhere [25]. The effects of higher adiabatic flame temperature due to heating and high oxygen concentration in the oxidizer flow in the present experiments are evident from the much higher extinction strain rates reported under the present conditions.

Extinction strain rates for liquid fuels, as functions of pressure, are shown in Figs. 5–8. Note that the scale of the liquid fuel plots is different from that for the gaseous fuels, reflecting the considerably lower extinction strain rates observed. Although fuel kinetic differences may play a role, much of the difference between the gaseous and liquid fuel data sets can be explained by the higher adiabatic flame temperatures of the gaseous fuels under the conditions investigated. Stoichiometric mixture fractions also differ significantly between the gaseous fuels (values of 0.12–0.13) and the liquid fuel vapor and N_2 mixtures (values of 0.42–0.45). However, this effect

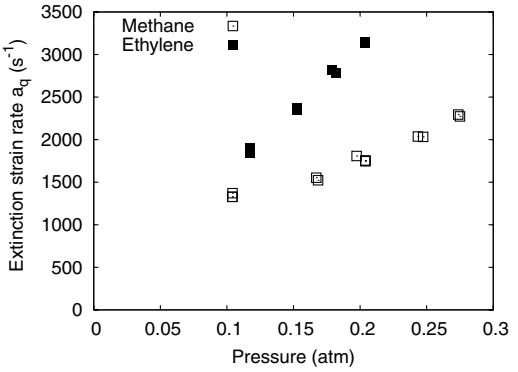

Fig. 4 Extinction strain rates for ethylene and methane as a function of pressure. The fuels were undiluted, and the oxidizer was a 50/50 molar blend of oxygen and nitrogen.

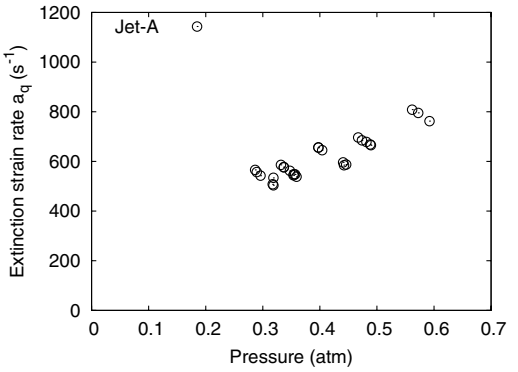

Fig. 5 Extinction strain rate of Jet-A as a function of pressure. The fuel was diluted in nitrogen to a mass fraction of 0.215, and the oxidizer was a 50/50 molar blend of oxygen and nitrogen.

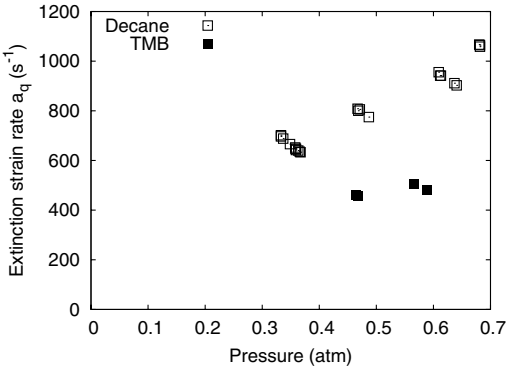

Fig. 6 Extinction strain rates of *n*-decane and TMB as functions of pressure. The fuels were diluted in nitrogen to a mass fraction of 0.215, and the oxidizer was a 50/50 molar blend of oxygen and nitrogen.

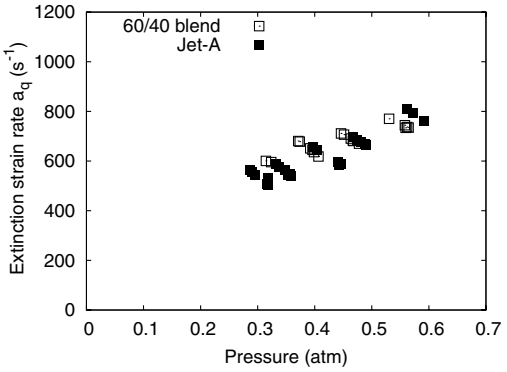

Fig. 7 Extinction strain rates of Jet-A and a 60/40 (by liquid volume) blend of *n*-decane and TMB, as functions of pressure. The fuels were vaporized into nitrogen to a mass fraction of 0.215, and the oxidizer was a 50/50 molar blend of oxygen and nitrogen.

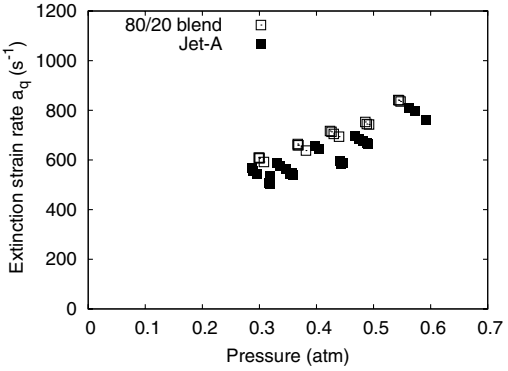

Fig. 8 Extinction strain rates of Jet-A and a 80/20 (by liquid volume) blend of *n*-decane and TMB, as functions of pressure. The fuels were vaporized into nitrogen to a mass fraction of 0.215, and the oxidizer was a 50/50 molar blend of oxygen and nitrogen.

cannot explain the qualitative difference between the gaseous and liquid fuel data sets. In fact, increasing the stoichiometric mixture fraction has been observed [24] to increase the extinction strain rate for a given fuel, when fuel- and air-side diluents are adjusted to maintain a constant adiabatic flame temperature.

Differences among the liquid fuels can be attributed largely to chemical kinetic effects, as we have matched adiabatic flame temperatures and stoichiometric mixture fractions to within a narrow range (see Table 2). Taking extinction strain rate as an indicator of overall reaction rate, we can rank the liquid fuels, with decane exhibiting the highest overall reaction rate and TMB the lowest. The higher overall reaction rate of a straight-chain alkane, in comparison to an aromatic compound, is consistent with the literature. Humer et al. [2] investigate flame extinction of *n*-decane and the aromatics toluene and xylene, which differ from TMB only in the number of methyl groups attached to the benzene unit. They report extinction strain rates for *n*-decane over a factor of 2 higher than those of the aromatics, when the mass fraction of each fuel was kept the same. Under engine ignition conditions, the higher reaction rates of alkanes vs aromatics have also been widely reported in studies of gasoline components [26].

The relative reactivities of *n*-decane and trimethyl benzene are also explained by thermochemistry. The secondary radicals initially formed from the normal alkane (*n*-decane) rapidly undergo beta scission reactions to form smaller olefins and alkyl radicals that propagate the radical pool. The alkyl radicals formed from the alkane also react rapidly with the O_2 molecule to form a mix of peroxy radicals, epoxides, and olefins, along with the radicals OH and HO_2. The pathways are different and yield fewer radicals in the case of trimethyl benzene. Methyl-substituted aromatics such as trimethyl benzene form benzyl radicals because of the weak C-H bonds on the methyl groups. These initially formed benzyl radicals do not undergo beta scission (elimination) reactions, because such reactions would require high endothermicity in that they involve ring opening and loss of the aromatic resonance. While the aromatic benzyl radicals readily react with O_2, the resulting benzyl peroxy radicals are highly unstable relative to alkyl peroxy radicals. For example, at 1000 K, they will react back to benzyl plus O_2 in less than a nanosecond, effecting a nonreaction. In blends, the methyl-substituted aromatics also serve to cap levels of the active alkane radical because of the much weaker C-H bond on the aromatic methyl group (90 kcal/mol) versus the primary and secondary C-H bonds on the alkyl molecule (98.5 and 101 kcal/mol). Through exothermic reactions such as the following, the reactions of the alkanes are shown:

$$\mathrm{CH_3\text{-}C_yC_6H_5 + CH_3CH \cdot CH_2CH_3 = C \cdot H_2C_yC_6H_5 + CH_3CH_2CH_2CH_3}$$

In this reaction, C_y refers to a cyclic compound or group. Radical sites are designated by the symbol ·. The enthalpy of reaction of the reaction listed is $\Delta H_{rxn} = -8.5$ kcal/mol.

As expected, the two blends of *n*-decane and TMB exhibit extinction characteristics between those of the pure fuels. Jet-As extinction strain rate also falls between the extreme values corresponding to the reference fuels. Extinction strain rates for two blends of decane and TMB (60/40 and 80/20 by liquid volume) are compared to Jet-A extinction strain rates in Figs. 7 and 8. While both blends have extinction behaviors very similar to those of Jet-A, the 60/40 blend behavior simulates that of Jet-A slightly better than does the 80/20 blend.

At each nominal pressure in Figs. 4–8, reactant mass flow rates were held constant and extinction was approached by progressively straining the flame through reduction of chamber pressure. So data points corresponding to multiple realizations of extinction strain rate

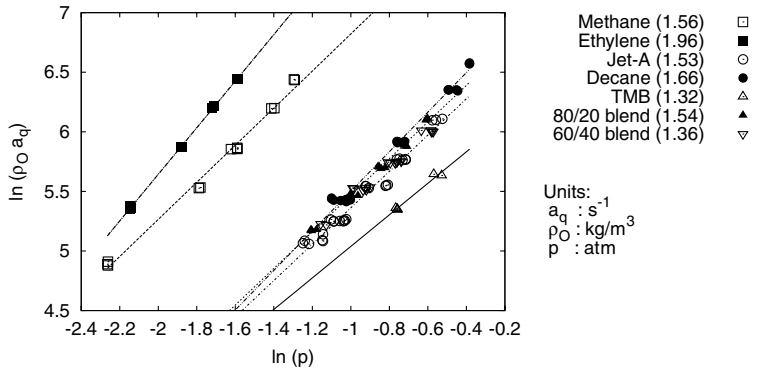

Fig. 9 Density scaling of extinction data, following Chelliah et al. [18]. Global reaction orders are reported in parentheses in the legend.

measurement reflect the inverse relationship between strain rate and chamber pressure required by Eq. (1).

B. Overall Reaction Order

The extinction strain rates measured for the gaseous and liquid fuels discussed above are replotted in density-weighted form in Fig. 9. Each extinction strain rate is multiplied by ρ_O, the oxidant density at the burner exit, which varies from point to point in the current study only when the pressure changes. The slope of a log/log plot of density-weighted extinction strain rate is an estimate of the overall reaction order, according to Chelliah et al. [18] and Law [19].

The reaction orders obtained here vary from 1.32 to almost 1.96 and appear to be basically independent of pressure for a given fuel, over the ranges investigated. Aside from ethylene (reaction order 1.96), the values obtained here are in a fairly narrow range (between 1.32 and 1.66). TMB and the blend containing the largest amount of TMB exhibit the lowest values of reaction order. The values substantially below two can be interpreted as indicating the increased importance of termolecular radical termination reactions as pressure increases, in the range of pressures investigated here [13].

VI. Conclusions

Opposed-jet diffusion flame extinction experiments have been performed over a range of subatmospheric pressures for several vaporized liquid fuels diluted in nitrogen and for pure methane and ethylene. The liquid fuel conditions were selected to match adiabatic flame temperature and stoichiometric mixture fraction. We have observed monotonic increases in extinction strain rates with pressure for each fuel and have extracted estimates of overall reaction order for the different fuels, ranging from 1.32 to 1.96. Under the conditions of the present study, we have demonstrated that a blend of *n*-decane and 1, 2, 4-trimethyl benzene is a good surrogate for Jet-A. Jet-A comprises several hundred compounds in varying proportions. Besides quantifying the dependence of its extinction strain rate on pressure, an objective of this study was to develop surrogates for it that had a manageable number of chemical components but were still representative of its burning characteristics. Decane has roughly the same carbon number as Jet-A, and TMB is representative of the aromatic content in Jet-A. Blending these two pure fuels in a suitable proportion would be expected to mimic Jet-A behavior. From a comparison of the extinction strain rates of Jet-A and the 60/40 blend of decane and TMB shown in Fig. 7, it is seen that for the entire range of pressures explored, there is little difference in the measured global extinction strain rates of these fuels, and hence the latter fuel lends itself to the possibility of serving as a surrogate for Jet-A.

Acknowledgments

The authors wish to acknowledge the support of the U.S. Air Force under contract FA8650-06-C-2658; Dean Eklund, U.S. Air Force Research Laboratory (AFRL), was the Contract Monitor. The authors thank Tim Edwards (AFRL) for providing the Jet-A fuel used in the study. The authors thank Christopher Montgomery (Reaction Engineering International) and Adel Sarofim (University of Utah) for useful discussions. Ryan Jacobs, Evan Respault, and Xin Zheng provided assistance with experiments.

References

[1] Colket, M., Edwards, T., Williams, S., Cernansky, N. P., Miller, D. L., Egolfopoulos, F. N., Lindstedt, P., Seshadri, K., Dryer, F. L., Law, C. K., Friend, D., Lenhert, D. B., Pitsch, H., Sarofim, A., Smooke, M. D., and Tsang, W., "Development of an Experimental Database and Kinetic Models for Surrogate Jet Fuels," 45th AIAA Aerospace Sciences Meeting and Exhibit, AIAA Paper 2007-770, 2007.

[2] Humer, S., Frassoldati, A., Granata, S., Faravelli, T., Ranzi, E., Seiser, R., and Seshadri, K., "Experimental and Kinetic Modeling Study of Combustion of JP-8, Its Surrogates and Reference Components in Laminar Nonpremixed Flows," *Proceedings of the Combustion Institute*, Vol. 31, Combustion Inst., Pittsburgh, PA, 2007, pp. 393–400.

[3] Cooke, J. A., Belluccia, M., Smooke, M. D., Gomez, A., Violi, A., Faravelli, T., and Ranzi, E., "Computational and Experimental Study of JP-8, a Surrogate, and Its Components in Counter-Flow Diffusion Flames," *Proceedings of the Combustion Institute*, Vol. 30, Combustion Inst., Pittsburgh, PA, 2005, pp. 439–446.

[4] Holley, A. T., Dong, Y., Andac, M. G., and Egolfopoulos, F. N., "Ignition and Extinction of Nonpremixed Flames of Single-Component Liquid Hydrocarbons, Jet Fuels, and Their Surrogates," *Proceedings of the Combustion Institute*, Vol. 31, Combustion Inst., Pittsburgh, PA, 2007, pp. 1205–1213.

[5] Peters, N., *Turbulent Combustion*, Cambridge Univ. Press, New York, 2000.

[6] Pellett, G. L., Convery, J., and Wilson, L. G., "Opposed Jet Burner Approach for Characterizing Flameholding Potentials of Hydrocarbon Scramjet Fuels," AIAA/ASME/SAE/ASEE 42nd Joint Propulsion Conference, Vol. 11, AIAA, Reston, VA, 2006, pp. 8717–8742.

[7] Mercier, R. A., and Ronald, T. M. F., "US Air Force Hypersonic Technology Program (HyTech)," AIAA International Space Planes and Hypersonic Systems and Technologies Conference, Norfolk, VA, AIAA Paper 1998-1566, 1998.

[8] Jackson, T., "Power for a Space Plane," *Scientific American*, Vol. 295, 2006, pp. 56–63.

[9] Colket, M., and Spadaccini, L., "Scramjet Fuels Autoignition Study," *Journal of Propulsion and Power*, Vol. 17, 2001, pp. 315–323. doi:10.2514/2.5744

[10] Cheng, S. I., "Hypersonic Propulsion," *Progress in Energy and Combustion Science*, Vol. 15, 1989, pp. 183–202. doi:10.1016/0360-1285(89)90008-7

[11] Tishkoff, J., Drummond, J., Edwards, T., and Nejad, A., "Future Direction of Supersonic Combustion Research—Air Force/NASA Workshop on Supersonic Combustion," 35th Aerospace Sciences Meeting and Exhibit, AIAA Paper 1997-1017, Reno, NV, 1997.

[12] Chang, A. Y., Bozzelli, J. W., and Dean, A. M., "Kinetic Analysis of Complex Chemical Activation and Unimolecular Dissociation Reactions Using QRRK Theory and the Modified Strong Collision Approximation,"*International Journal of Research in Physical Chemistry and Chemical Physics*, Vol. 214, 2000, pp. 1533–1568. doi:10.1524/zpch.2000.214.11.1533

[13] Law, C. K., "Propagation, Structure and Limit Phenomena of Laminar Flames at Elevated Pressures," *Combustion Science and Technology*, Vol. 178, 2006, pp. 335–360. doi:10.1080/00102200500290690

[14] Papas, P., Glassman, I., and Law, C. K., "Effects of Pressure and Dilution on the Extinction of Counterflow Nonpremixed Hydrogen-Air Flames," *Proceedings of the Combustion Institute*, Combustion Inst., Pittsburgh, PA, 1994, p. 1333.

[15] Sohn, C. H., and Chung, S. H., "Effect of Pressure on the Extinction, Acoustic Pressure Response, and NO Formation in Diluted Hydrogen-Air Diffusion Flames," *Combustion and Flame*, Vol. 121, 2000, pp. 288–300. doi:10.1016/S0010-2180(99)00140-6

[16] Glassman, I., *Combustion*, Academic Press, New York 1996.

[17] Pons, L., Darabiha, N., and Candel, S., "Pressure Effects on Nonpremixed Strained Flames," *Combustion and Flame*, Vol. 152, 2008, pp. 218–229. doi:10.1016/j.combustflame.2007.07.006

[18] Chelliah, H. K., Law, C. K., Ueda, T., Smoke, M. D., and Williams, F. A., "An Experimental and Theoretical Investigation of the Dilution, Pressure and Flow-Field Effects on the Extinction Condition of Methane-Air-Nitrogen Diffusion Flames," *23rd Symposium on Combustion*, Combustion Inst., Pittsburgh, PA, 1990, pp. 503–511.

[19] Law, C. K., "Extinction of Counterflow Diffusion Flames with Branching-Termination Chain Mechanisms: Theory and Experiment," *Mathematical Modelling in Combustion Science*, edited by, J. D. Buckmaster, and T. Takeno, Springer–Verlag, Berlin, 1987.

[20] Edwards, T., "Cracking and Deposition Behavior of Supercritical Hydrocarbon Aviation Fuels," *Combustion Science and Technology*, Vol. 178, 2006, pp. 307–334. doi:10.1080/00102200500294346

[21] Sveen, J. K., "An Introduction to MatPIV v.1.6.1," Eprint No. 2, Dept. of Mathematics, Univ. of Oslo, Oslo, 2004.

[22] Seshadri, K., and Williams, F. A., "Laminar Flow Between Parallel Plates with Injection of a Reactant at High Reynolds Number," *International Journal of Heat and Mass Transfer*, Vol. 21, 1978, pp. 251–253. doi:10.1016/0017-9310(78)90230-2

[23] Zegers, E. J. P., Williams, B. A., Fisher, E. M., Fleming, J. W., and Sheinson, R., "Suppression of Nonpremixed Flames by Fluorinated Ethanes and Propanes," *Combustion and Flame*, Vol. 121, 2000, pp. 471–487.

doi:10.1016/S0010-2180(99)00162-5
[24] Chen, R., and Axelbaum, R. L., "Scalar Dissipation Rate at Extinction and the Effects of Oxygen-Enriched Combustion," *Combustion and Flame*, Vol. 142, 2005, pp. 62–71. doi:10.1016/j.combustflame.2005.02.008
[25] Dattarajan, S., Montgomery, C. J., Gouldin, F. C., Fisher, E. M., and Bozzelli, J. W., "Extinction of Opposed Jet Diffusion Flames of Scramjet Fuel Components at Subatmospheric Pressures," 46th Aerospace Sciences Meeting and Exhibit, AIAA Paper 2008-0996, Reno, NV, 2008.
[26] Golombok, M., Kalghatgi, G. T., and Tindall, A., "Heat Release and Knock in Paraffinic and Aromatic Fuels and the Effect of an Ashless Anti-Knock Additive," Society of Automotive Engineers Paper 952405, 1995.

J. Gore
Associate Editor